Separation Science and Technology
Publication details, including instructions for authors and subscription information:
http://www.informaworld.com/smpp/title~content=t713708471

Dynamics and Rheology of Fouling Cakes Formed During Ultrafil Tration

Sandip Datta[a]; J. Leo Gaddis[a]
[a] Department of Mechanical Engineering, Clemson University, Clemson, SC, USA

To cite this Article Datta, Sandip and Gaddis, J. Leo(1997) 'Dynamics and Rheology of Fouling Cakes Formed During Ultrafil Tration', Separation Science and Technology, 32: 1, 327 — 353
To link to this Article: DOI: 10.1080/01496399708003202
URL: http://dx.doi.org/10.1080/01496399708003202

SEPARATION SCIENCE AND TECHNOLOGY, 32(1-4), pp. 327-353, 1997

DYNAMICS AND RHEOLOGY OF FOULING CAKES FORMED DURING ULTRAFILTRATION

SANDIP DATTA & J. LEO GADDIS

Department of Mechanical Engineering
Clemson University, Clemson, SC 29634, USA

ABSTRACT

The solute cake which forms on a membrane surface during ultrafiltration processes is well known for its fouling characteristics. The dynamics and rheology of the cake are investigated and observed under the action of cross-flow shear. Experiments with slurries having 300 nm diameter particles of titanium dioxide indicate average volume concentrations of 0.56 or 0.57 and show that this cake indeed 'flows' with a creeping velocity under applied shear. The cake thickness reaches a steady state when the solute advection towards the membrane balances the solute mass carried away at the trailing edge by the creeping cake. The viscosity-shear rate dependence of this layer is determined experimentally and the 'creeping velocity' of the cake is calculated assuming the transverse drag force is determined from the Kozeny-Carman equation. Upon instantaneous compression the cake compresses while maintaining its mass distribution. The change in cake resistance allows interpretation of the pressure modified concentration. The volume concentration, determined from the mathematical modeling, is shown to lie between 0.54 to 0.65. Observations show that the top few layers of this cake move freely with the shearing flow due to the lifting action of normal stresses in the cake under external shear. Volume concentrations up to 0.65 are indicated from the analysis.

INTRODUCTION

Consider a cross-flow ultrafiltration process where the shear stress is applied by the flow rate of the bulk solution (slurry) over a flat membrane. The membrane is supposed to exhibit perfect rejection. The slurry particles when compressed in a cake experience a drag force due to the permeate flow rate. This drag force pushes the particles towards the membrane and compresses the cake. This drag force is

responsible for stabilizing the cake against external disturbances and increasing the permeate flow resistance. The cake gets compacted and its viscosity increases, thus decreasing the creeping velocity of flow. This drag pressure can be estimated from the Kozeny-Carman Equation (1). There are other models (2) which calculate the drag force through a bed of particles. Near the edge of a cake the resistance to flow is like single particles or collection of particles. Happel and Brenner (3) give an excellent discussion of drag calculation for two to four spheres freely falling in a viscous liquid. The drag force is similar to Stokes' drag but with a correction factor which is dependent on their separation distances, their radii, and whether or not they are free to rotate. The drag force due to Happel and Brenner can be applied to the top few layers of the cake, where the absence of other particles above precludes any other particle-particle interaction that may occur.

Saffman (4) discussed the lift of a small sphere in a slow shear flow. He showed that the lift deflects and acts on the particles perpendicular to the flow direction. Saffman also discussed the relevance of the results to the observations of Segré and Silberberg (5) of small spheres in Poiseuille flow.

Saffman's constant was predicted as 16.1 and subsequently modified to 81.2. Soo (6) calculated the constant to be 6.46 by numerical integration. Saffman showed that unless the rotating speed is very much greater than the rate of shear for a freely rotating particle with angular velocity as given by Einstein' s equation, the lift force due to the particle rotation is less by an order of magnitude than that due to shear (7). This conclusion is valid when the Reynolds Number based on particle diameter is small. The dependence on viscosity is such that the drift velocity should be proportional to $Re^{(2/3)}$ if U(x) is independent of v. For a spinning particle this Magnus force can be significant (7).

The question arises whether the Saffman's force is active on particles in a packed bed of spheres. Saffman idealized his case by considering a single particle

in a shearing flow with boundaries at infinity. In our case however the particles are packed in a creeping cake and the top boundary of the flow is far from the initiated in detail by Hamaker (9), who investigated the attractive forces between spherical particles. He ascribed the common additive force phenomena between particles to the London-van der Waals interaction.

If the particles in the slurry are charged and separated by a solvent having electrolytic properties, electrostatic forces may be significant for calculation of repulsive (suspending) forces acting on the solute particles. The surface potential Ψ_0 with electrolyte concentration in the gap separating two planar surfaces having a surface charge density σ can be calculated from the Grahame Equation (8). It should be instructive to note that divalent or trivalent ion concentrations in the gap have a more drastic effect on the potential on the surface of the solid.

The charge density can also be expressed as equivalent to a capacitor whose plates are separated by a distance $1/\kappa_D$, have charge densities $\pm \sigma$ and the potential difference Ψ_0. This analogy with a charged capacitor gave rise to the name *diffuse electric double layer* for describing the ionic atmosphere near a charged surface whose characteristic length or thickness is known as the Debye length $1/\kappa_D$. The magnitude of the Debye length depends solely on the properties of the liquid and not on any property of the surface such as its charge or potential (8). The electrostatic double-layer interaction between charged surfaces in electrolyte was calculated by Israelachvili (8). As in the case of van der Waals forces this electrostatic force is also expressed as a force-distance model.

All the forces discussed above can be accommodated if one finds the lift force on the particles of a shearing slurry experimentally. One of the common characterizations of the lift force mechanism is that of the primary normal stress of a shearing slurry. The normal stress results from lift forces on particles of the slurry

when subjected to a shearing rate. This shearing rate is dependent on the local shear stress and viscosity of the slurry.

The viscosity μ (also called the non-Newtonian viscosity or shear rate dependent viscosity) is defined analogously to the viscosities for Newtonian fluids,

$$\tau_{yx} = -\mu\gamma_{yx};\ \mu = \mu(c,\gamma). \tag{2}$$

The primary normal stress coefficients Ψ_1 and Ψ_2 are defined as follows;

$$\tau_{xx} - \tau_{yy} = -\Psi_1(\gamma)\gamma_{yx}^2. \tag{3a}$$

$$\tau_{yy} - \tau_{zz} = -\Psi_2(\gamma)\gamma_{yx}^2. \tag{3b}$$

The functions Ψ_1 and Ψ_2 are known as the first and second normal stress coefficients, respectively; μ, Ψ_1, and Ψ_2 are sometimes collectively referred to as the viscometric functions (10, 11).

The primary normal stresses can be determined experimentally or can be estimated from shear-viscosity data. Normal stresses can be calculated from shear viscosity data using for example, Abdel-Khalik, Hassager, Bird model (AKHB) (12) or Wagner (13) model. The AKHB model is given by

$$\Psi_1(\beta) = \frac{4K_A}{\pi}\int_0^\infty \frac{\mu(\beta) - \mu(x)}{x^2 - \beta^2}dx \tag{4}$$

where Ψ_1 is expressed as a function of the shear rate β. The main disadvantage of this model is the improper integral in Equation (4). A similar model was proposed by Wagner (13) as,

$$\Psi_1(\beta) = -\frac{1}{N}\frac{d\mu(\beta)}{d\beta}. \tag{5}$$

In our experiment with titania (rutile TiO_2) powder, the viscosity of the slurry followed a power law model. Thus one can express the viscosity of the slurry as Equation (6)

$$\mu - \mu_\infty = m\gamma^{n-1} \tag{6}$$

where μ_∞ is the viscosity at infinite shear rate, m is a parameter with dimension of Pa-s^n, while n is a dimensionless parameter. For Newtonian fluids n=1, μ_∞=0 and m is the viscosity. When n<1, the fluid is said to be pseudoplastic or shear thinning, while if n>1 the fluid is said to be dilatant or shear thickening.

There are many models of the concentration dependence for the viscosity of slurries. These viscosity-concentration models are useful in determining the cake viscosity and ultimately determining its creeping velocity. Some of the models widely available in the literature are indicated in Table 1. Note in all these models viscosity is only a function of the slurry volume concentration. Therefore all these models are valid for shear-independent regimes. One expects the slurry viscosity to be a function of the cake concentration and the impressed strain rate as well.

Some of the force models under discussion are force-distance; while others are pressure (stress)-concentration models. For comparison purposes one model can be transformed to the other by knowledge of geometry of the particle agglomeration. There are many geometric interpretations for estimation of packing densities (volume concentrations) of rigid spheres (19, 20, 21, 22). The most logical choice is the tetrahedral packing (22) with the interparticle distance being such as to make the average volume concentration to be 0.58-0.60, the volume concentration for loose random particle packing. Though the maximum volume membrane compared to the particle size and cake dimensions. The particles are sheared in a slow shear flow (creeping) and the only criterion which is difficult to consider here is the effect of other particles nearby. It can be safely assumed that the presence of other particles will break up the flow streamlines and at most decrease this lift force and not increase it.

Rubinow and Keller (7) computed the transverse force on a spinning sphere moving in a viscous fluid. The calculation was based on small values of Reynolds number. For small values of the Reynolds number, this lift force is independent of

TABLE 1.COMPARISON OF DIFFERENT VISCOSITY MODELS.

Viscosity Models	Equation	Comments
Einstein (14)	$\mu=\mu_0(1+2.5c)$	$c \leq 0.15$
Batchelor (15)	$\mu=\mu_0(1+2.5c+6.2c^2)$	$c \leq 0.15$
Mooney (16)	$\frac{\mu}{\mu_0} = \exp\left(\frac{acc_{max}}{c_{max}-c}\right)$	a=2.5, c_{max}=0.74, c≥0.15
Dougherty-Krieger (17)	$\mu = \mu_0\left(1 - \frac{c}{c_{max}}\right)^{-a\,c_{max}}$	a=2.5, c_{max}=0.74, c≥0.15
Leighton-Acrivos (18)	$\frac{\mu}{\mu_0} = \left[1 + \frac{0.5ac}{1-\frac{c}{c_{max}}}\right]^2$	a=3.0, c_{max}=0.58 c≥0.15

the fluid viscosity. Again the question arises whether the presence of other particles alters this lift force. As before it can be argued that the presence of other particles in the vicinity can only reduce this force and never increase it, since other particles will break up the streamlines of the flow and thus the effective force experienced by a particle will only decrease.

According to Zydney and Colton (1) the pressure drop due to Kozeny-Carman drag due to flow through a packed bed having uniform volume concentration C_c and thickness δ and comprising of rigid non interacting spheres of radius R can be expressed as

$$\Delta P = \frac{9KJ\mu_0}{R^2}\frac{C_c^2\delta}{(1-C_c)^3}; \quad \frac{dP}{dy} = r\,J. \tag{1}$$

Here r is the resistivity of the bed and K is the Kozeny-Carman constant. Generally this constant takes a value between 5 and 7, but other values of K cannot be ruled out. Here J is the volume flux through this packed bed and μ_0 the solvent viscosity.

Van der Waals forces play a potentially significant role in all phenomena

involving particles at close spacings. They may not be as strong as Coulombic (electrostatic) forces, nevertheless they are present irrespective of the surface electrostatic charge configuration of the particles. Israelachvili (8) added to studies concentration for ordered particle arrays can reach 0.7796 (19), in practice it is difficult to reach a packed volume concentration beyond a value of 0.68.

Once the array geometry has been suitably estimated, the interparticle distance can be obtained from the volume concentration of the packing and the pressure acting on one particle can be expressed in terms of inter-particle forces, which the neighboring particles experience. The order of magnitude for all the above forces for 300 nm particles under 20 Pa of shear is determined. It was assumed that the average cake concentration was 0.57 and the thickness was 100 μm. Table 2 shows the maximum possible values of these forces under our operating conditions.

THEORY

A membrane is located at y = 0 adjacent to a fluid in the region y>0 and extracts permeate from x = 0 to x = L. Define a volume of unit depth from x to x+Δx and from y = 0 to y = h > δ, δ being the local instantaneous cake thickness. The permeate exits with velocity J in the negative y-direction and fluid enters the top of the volume at velocity v_T. Conservation of solute, after division by density of particle, for the designated volume is

$$\int_0^h C(x,y)u(x,y)dy - \int_0^h C(x+\Delta x,y)u(x+\Delta x,y)dy + v_T C_0 \Delta x = \left[C(x,\delta)-C_0\right]\frac{\partial \delta}{\partial t}\Delta x. \tag{7a}$$

A similar equation for the solvent phase is

$$\int_0^h \left[1-C(x,y)\right]u(x,y)dy - \int_0^h \left[1-C(x+\Delta x,y)\right]u(x+\Delta x,y)dy + v_T\left[1-C_0\right]\Delta x - J\Delta x = -\left[C(x,\delta)-C_0\right]\frac{\partial \delta}{\partial t}\Delta x. \tag{7b}$$

TABLE 2. RELATIVE MAGNITUDE OF ALL NORMAL FORCES/STRESSES.

Force /Pressure	Max Magnitude	Comments
Saffman	$6.2*10^{-11}$ N	lift on single particle
Rubinow and Keller	2.810^{-13} N	lift on single particle
van der Waals	$2*10^{-9}$ N	attractive
Electric Double Layer	$2*10^{-8}$ N	σ=-0.2 C/m^2, 10^{-7} molar
Happel and Brenner	$6.57*10^{-14}$ N	particles free to rotate
"	$6.68*10^{-14}$ N	particles not free to rotate
Kozeny-Carman Drag	$2.7*10^{4}$ Pa	C_c =0.57, J =$3*10^{-5}$ m/s
Primary Normal Stress	$1.3*10^{3}$ Pa	maximum occurs at conc.0.3-0.37

Equations (7a) and (7b) may be multiplied respectively by $1-C_0$ and C_0 and combined to eliminate v_T, resulting in

$$\int_0^h [C(x,y)-C_0]u(x,y)dy - \int_0^h [C(x+\Delta x,y)-C_0]u(x+\Delta x,y)dy + J\Delta xC_0 = [C(x,\delta)-C_0]\frac{\partial \delta}{\partial t}\Delta x. \quad (8)$$

Clearly the integrals in Equation (8) vanish for $y > \delta$, since there $C(x,y) = C_0$. These integrals represent the excess solute flow at a position over and above the flow at the bulk concentration. The term $J\Delta xC_0$ represents the solute added and the term on the right is the solute which must accumulate in the cake.

It is supposed that the cake layers will exist in a region of constant shear stress, and that the viscosity of the cake will depend only on the local concentration of the cake. In such a case the velocity, u(x,y), of crossflow in the x-direction will be according to Equation (9)

$$u(x,y) = \frac{I(x,y)}{\mu_0}, \text{ where } I(x,y) = \int_0^y \tau(x)\frac{\mu_0}{\mu(c,\tau)}dy. \tag{9}$$

Expansion of the integral at x+Δx of Equation (8) in terms of variables at x and use of the Leibnitz procedure for differentiation allows Equation (8) to become

$$[C(x,\delta)-C_0]\frac{\partial\delta}{\partial t} + \frac{d}{dx}\int_0^\delta \frac{[C(x,y)-C_0]I(x,y)}{\mu_0}dy = JC_0. \tag{10}$$

It is straightforward to simplify this equation for a constant shear stress and constant cake concentration which also implies constant viscosity. The solution for thickness as a function of time and position for constant concentration layers may be accomplished by standard methods. Either the flux must be prescribed or the pressure prescribed together with a model for the resistivity of the cake and resistance of the membrane.

If the cake concentration is considered non-uniform there must be some model to define the relation of concentration to external stimulus. Such stimuli could include applied normal stress, shear stress, solution pH, and electrolyte concentration. In the cakes envisioned herein the applied normal stress at any point is taken to be the accumulated pressure from the solvent pressure loss induced by its passage through the portion of cake from its edge. This stress is modeled to correspond to a single value of concentration.

The creeping cake described here is a packed bed of spheres which are solute particles in the slurry. If the cake concentration is variable, say C(x,y), then the pressure drop ΔP(x,y) due to Kozeny-Carman drag at any location can be estimated to be

$$\frac{\partial P}{\partial y} = \frac{9KJ(x)\mu_0}{R^2}\frac{C(x,y)^2}{(1 - C(x,y))^3}; \quad \Delta P(x,y) = \int_{\delta(x)}^{y} \frac{9KJ(x)\mu_0}{R^2}\frac{C(x,y')^2dy'}{(1 - C(x,y'))^3}. \tag{11}$$

Also $\Delta P(x,0) = \Delta P(x)_{total} - R_m J(x)$, where $\Delta P(x)_{total}$ is the total pressure drop from the feed to the permeate side at any location x. Here $\Delta P(x,0)$ is the trans-cake pressure drop and $R_m J(x)$ is the pressure drop across the membrane.

For constant cake concentration C_c and constant shear stress τ Equation (11) can be simplified and for the Kozeny-Carman drag relationship Equation (12) can be obtained.

$$\frac{\Delta P}{R_m + r\delta(x,t)} = J(x,t);\ r = \frac{9K\mu_0 C_c^2}{R^2(1 - C_c)^3} \tag{12}$$

where r is the hydraulic resistivity of the bed of particles.

At steady state the flux $\delta(x)$ and $J(x)$ can be obtained from the above equations as

$$\frac{\tau}{\mu_c}\left[R_m\frac{\delta^2}{2} + r\frac{\delta^3}{2}\right] = \Delta P\frac{C_0}{C_c - C_0}x \tag{13}$$

and

$$\left[x - \left(\frac{\tau}{\mu_c 6r^2}\left(\frac{C_c - C_0}{C_0}\right)\right)\frac{R_m^3}{\Delta P}\right]J^3 + \left(\frac{\tau}{\mu_c 6r^2}\left(\frac{C_c - C_0}{C_0}\right)\right)(3R_m\Delta P)J - 2\left(\frac{\tau}{\mu_c 6r^2}\left(\frac{C_c - C_0}{C_0}\right)\right)\Delta P^2 = 0. \tag{14}$$

In the transient phase as the cake accumulates the solute available in the bulk slurry decreases and therefore C_0 in Equations (13) and (14) may be different from the initial value of C_0. From Equation (14) the flux distribution J(x), (i.e., variation of flux with longitudinal distance x) can be calculated. Subsequently the mean flux $\bar{J}$ can be obtained as

$$\bar{J} = \frac{1}{L}\int_0^L J(x)\,dx. \tag{15}$$

This mean flux can be verified with experimental data of permeate flux. From Equation (14) $J \sim x^{-0.33}$ when $r\delta >> R_m$, the usual 1/3 power dependence. The mass balance equation at any longitudinal location (x) is given by the following equation.

$$\int_0^x J(x')\ C_0\ dx' = \int_0^{\delta(x)} u(x,y)\ (C(x,y) - C_0)\ dy. \tag{16}$$

The mass balance in Equation (16) also dictates that at the steady state the mass of solute advected towards the membrane should exactly balance the solute mass flowing out due to creeping velocity of the cake. Thus the three variables $\delta(x)$, $J(x)$ and C_c can be determined for the steady state condition. The creeping velocity of the cake can be obtained from Equation (9) for a constant cake concentration C_c and with $y \leq \delta(x)$.

It is relevant to mention here the effect of the primary normal stresses. The authors expect the stresses to be exerted on the particles in the slurry and further that on top of any dense cake layer a suspended cloudy layer of particles will form balancing the local Kozeny-Carman drag by the lift forces represented by these stresses. For this case the volume concentration of this cloudy layer is between 0.33-0.37 and it flows with a velocity of few millimeters per second. Though the thickness of this layer is only 4 to 5 μm, it carries a potentially substantial fraction of the total solute flow rate exiting that test section. For the situation at hand the cloudy layer bears a nearly negligible flow. The primary resistance and mass is estimated to be in the main region of the cake.

DATA INTERPRETATION AND EXPERIMENTATION

Viscosity measurements of a slurry of titanium dioxide particles in water were conducted for different solute concentrations and over a shear rate range. The titania particles were monodisperse spheres of diameter 300 nm and specific gravity of 4.26. A stock solution was created by high shear dispersion of volume concentration of 0.354 using 15.3 ml of dispersant *Nopcosperse 44* in 2203 ml of slurry. Water was allowed to evaporate from this slurry raising the concentration in steps to 0.548 by volume. The torque was measured in a concentric cylinder-

and-bob viscometer (Contraves Rheomat 30) under different strain rates. The data obtained are shown in Figure 1. These data were fitted for viscosities exhibited by a power law model as indicated, and from its characteristics, the primary normal stress coefficients are evaluated. The model for the first normal stress coefficients using Wagner model is indicated (Table 3). The parameters m, n and μ_∞ are tabulated in Table 3 for different concentrations of titania.

For titania slurries with the exception of one data point all values of n lie between n=0.1 and 0.2. The point which does not fall into the interval proposed by Wagner (13) is barely beyond the limit.

Ultrafiltration experiments with the same titania powder were conducted to study the transient and steady state behavior of the fouling cake formed on the membrane. All experiments were conducted at 40°C and all viscosity data were corrected in proportion to solvent viscosity for that temperature. A bulk volume concentration of $2*10^{-4}$ was used for all the experiments conducted with titania. A stainless steel flat porous metal (Mott Metallurgical Co. 0.5 μm rating) sheet was impregnated with titania slurry, dried and sintered at 2000°F. Two such flat membrane sections measuring 234 mm x 54 mm were subjected to cross flow ultrafiltration. The flow channel had dimensions of 54 mm x 3 mm. Pressure gauges upstream and downstream of the module measured the pressure drop along the length of the membrane. A pressure gauge mounted at the center of the membrane module read the average transmembrane pressure drop. A magnetic flowmeter measured the bulk flow rate which was, in turn, interpreted to estimate the shear stress of operation. An orifice flowmeter measured the permeate flow rate from which the transient and steady state flux were calculated. Two experiments were conducted with operating pressures of 0.259 and 0.241 MPa and shear stresses of 17 and 25 Pa respectively. The unfouled membrane resistances were

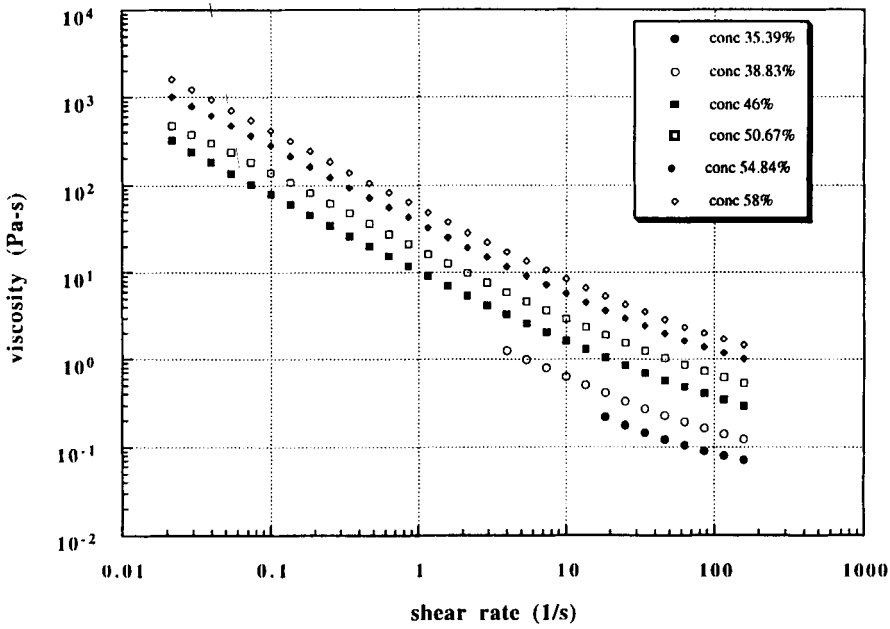

FIGURE 1. Viscosity of Titania Under Different Shear Rates.

TABLE 3.COMPARISON OF DIFFERENT PARAMETERS OF WAGNER MODEL AT DIFFERENT CONCENTRATIONS.

volume concentration	Power Law Model $\mu(\gamma)=\mu_\infty + m\gamma^{(n-1)}$			$\Psi_1(\gamma)=A\beta\gamma^{-C\beta}$	
	m	n	μ_∞	$A\beta$	$C\beta$
0.58†	55.755	0.1385	0.769	346.8082	1.8615
0.5485	37.472	0.1448	0.5326	221.3125	1.8552
0.5067	18.854	0.1548	0.2828	102.9419	1.8452
0.46	10.629	0.1466	0.6462	61.8744	1.8534
0.3883	3.5287	0.2105	0.0590	13.2347	1.7895
0.3539	2.238	0.1225	0.0457	16.0314	1.8775

† extrapolated from lower concentration values

$9.5*10^9$ and $3.5*10^9$ Pa-s/m respectively. The pH of the slurry was measured to be 10.41 and 10.62 respectively.

Once steady state was reached the effect of different pressures on the established cake was investigated. The transmembrane pressure drop was stepped from 0.241 to 0.655 MPa and back while maintaining the shear stress level. This pressure variation was done very quickly (in about 15 minutes), which ensured that negligible additional fouling or erosion of the cake occurred in that time period, which is reasonable since the time to reach a steady state cake thickness takes from 6-12 hours in the experiment conducted. From the flux data the cake resistivity was determined and the average cake concentration using the Kozeny-Carman relationship was evaluated.

RESULTS AND DISCUSSION

1) Interpretation of Extant Results

Porter's (23) flux data for suspensions were up to 38.5 times higher than predictions by a diffusion-based theory. The viscosity for his slurry of polystyrene latex is estimated from Mooney's Equation (Table 1) and average cake concentrations were estimated to fit his flux data at the indicated recirculation rates. The data sets selected for examination are:

a) styrene-butadiene polymer latex at constant pressure drop of 60 psi and bulk concentration varying from 0.05 to 0.5 volume concentration and recirculation rate varying from 5 to 40 gpm, and

b) styrene-butadiene polymer latex at constant recirculation rate of 11.8 gpm with bulk concentration varying from 0.01 to 0.2 and average transmembrane pressure drop varying from 20 to 93 psi.

If one applies for case (a) the creeping cake model (Equations 9, 12-16) the inferred cake concentration is shown in Figures 2 and 3. The cake concentration

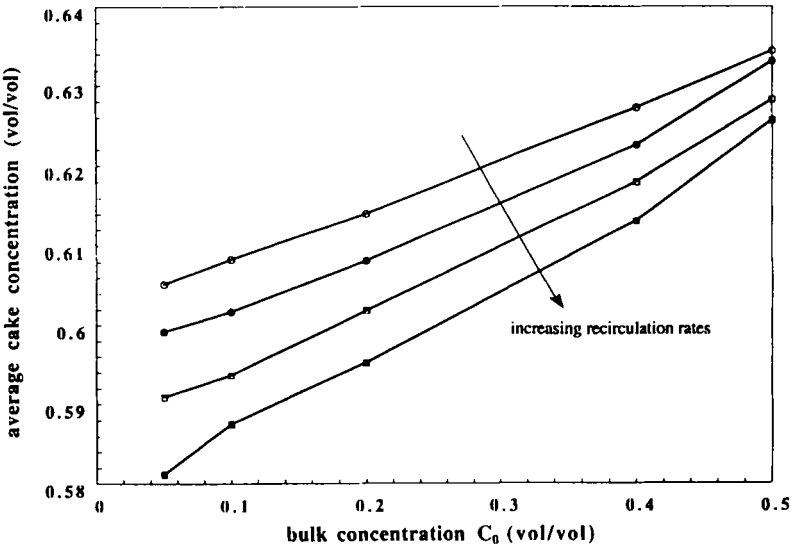

FIGURE 2. Average Cake Concentration Under Different Shear and Bulk Concentrations (Porter).

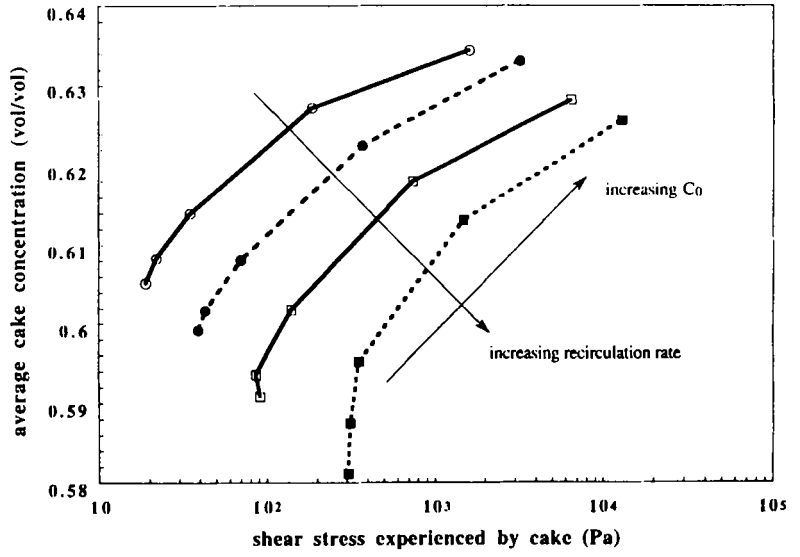

FIGURE 3. Average Cake Concentration Under Different Shear Rates (Porter).

for each operating point corresponds to the value which balances the mass flow towards the membrane with that sloughed off at the trailing edge of the creeping cake. The thickness distribution $\delta(x)$ of the cake is obtained from a balance of pressure with Kozeny-Carman drag and mass flow of the cake. This thickness (Equations 12 and 13) yields a distribution $J(x)$ whose average value is the observed mean flux. From Figure 2 it is apparent that higher bulk concentrations correspond to higher cake concentrations. The cake concentrations lie within a range of 0.58 to 0.64. These values are very close to the concentrations of random or close packed spherical particles. The concentration estimate is quite sensitive to the viscosity model used to correlate concentration with viscosity. Though Mooney's model (18) may be adequate for high strain rates (high shear stresses) it may underpredict the viscosity values at smaller strain rates. This inference can be drawn easily based on the experimental viscosity values for titania given in Figure 1. Figure 2 also shows that at constant bulk concentrations higher recirculation rates lower average cake concentration.

The variation of cake concentration with the bulk solution is almost linear for all the recirculation rates. If the shear stress is estimated by standard methods, Figure 3 results. Interpretation of the phenomena in terms of shear stress does not clearly diminish the complexity of dependence of the cake concentration on operating parameters.

For case (b) the recirculation was kept constant. The data from this set are shown in Figure 4 as the effect of strain rate in the cake on the cake concentration. The cake concentration can be expected to decline with increasing strain rate which dilates the cake dynamically. Because the recirculation rate here was kept constant, the shear stress at any concentration must also be constant. But strain rate varied with cake properties in response to the only other variable, pressure. The cake concentration varies with the total trans-cake pressure drop (Figure 5) as

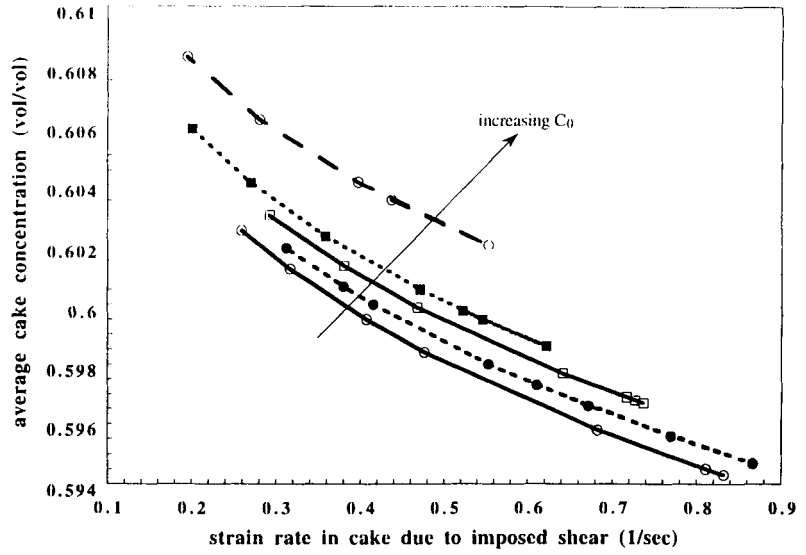

FIGURE 4. Average Cake Concentration Under Different Strain Rates and Bulk Concentrations (Porter).

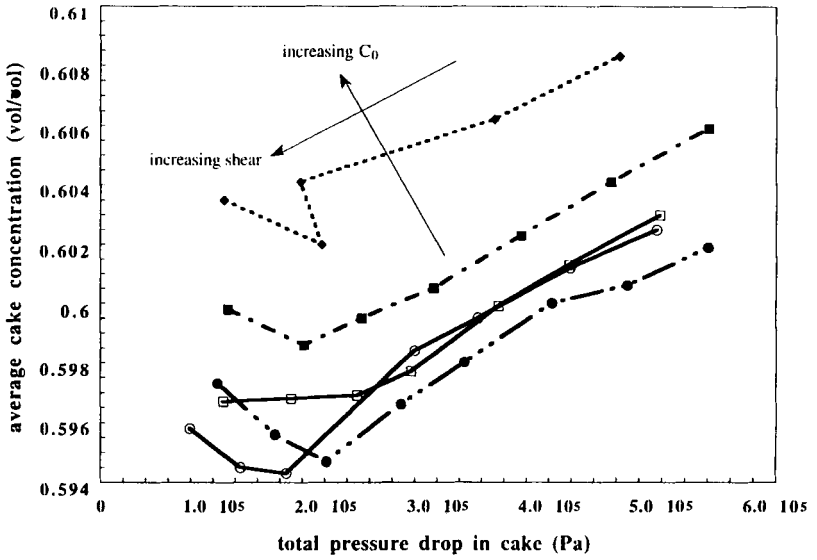

FIGURE 5. Average Cake Concentration as a Function of Cake Pressure Drop, Shear Stress and Bulk Concentration (Porter).

anticipated. Higher pressure causes a higher compaction of the cake. The range in average cake concentration for set (b) is much less for set (a). This is attributed to smaller range in shear stress and bulk concentration.

2) Interpretation of Current Results

Experiments with titania slurry were carried out; the viscosity data (Figure 1) were used to formulate predictions. Equation (10) was solved using a constant cake concentration C_c and a constant shear stress τ for the transient behavior and it can be seen from Figures 6 and 7 that experimental data and theoretical predictions agree quite well. The cake concentrations which match the theoretical prediction with the experimental value were 0.57 and 0.56, respectively, for the high resistance and low resistance membranes.

A cake was established virtually as shown in Figure 7 by a period of initial operation at a shear stress of 17 Pa and an operating pressure of 0.241 MPa. Once the steady state was reached, keeping the shear stress constant (same bulk flow rate) the pressure was changed in sequential steps from 0.241 Pa to 0.655 MPa and back. As indicated in Figure 8, little hysteresis was observed.

For the steady state condition i.e., the first point on Figure 8, a calculation of the solute mass excess integrals may be made as in Equation (16) or (8) at any pair of points, x and $x+\Delta x$. The right side of Equation (8) is zero for steady state. For a certain step Δx and the right side zero, the mean flux which agrees with the difference in the adjacent integrals may be computed. Stepping along the membrane allows the generation of $J(x)$ and $\delta(x)$, with $C(x,y)$ assumed at all interior points. This is the steady-state solution to the integral Equation (8). There are many concentrations $C(x,y)$ which satisfy this steady-state flux, pressure condition. Each produces different thickness distributions for the cake, however, the response of these cakes is vastly different for the excursion of Figure 8.

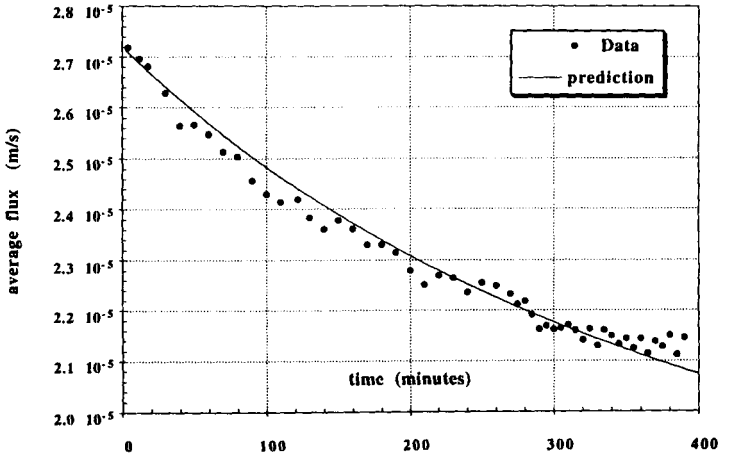

FIGURE 6. Transient Flux Variation for Titania Experiment, R_m=9.5*10^9 Pa-s/m.

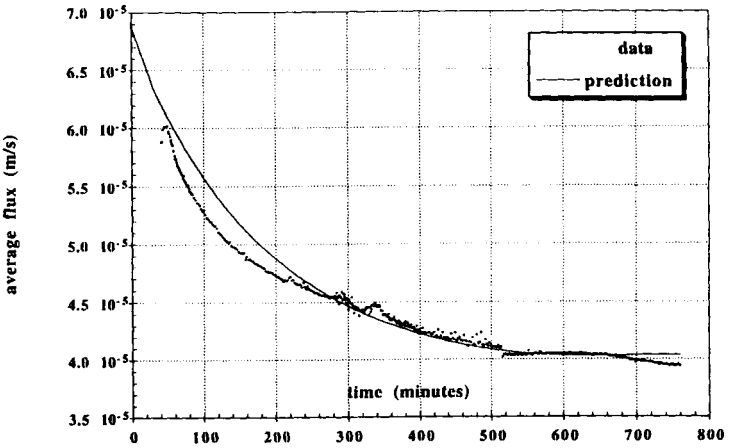

FIGURE 7. Transient Flux Variation for Titania Experiment, R_m=3.5*10^9 Pa-s/m.

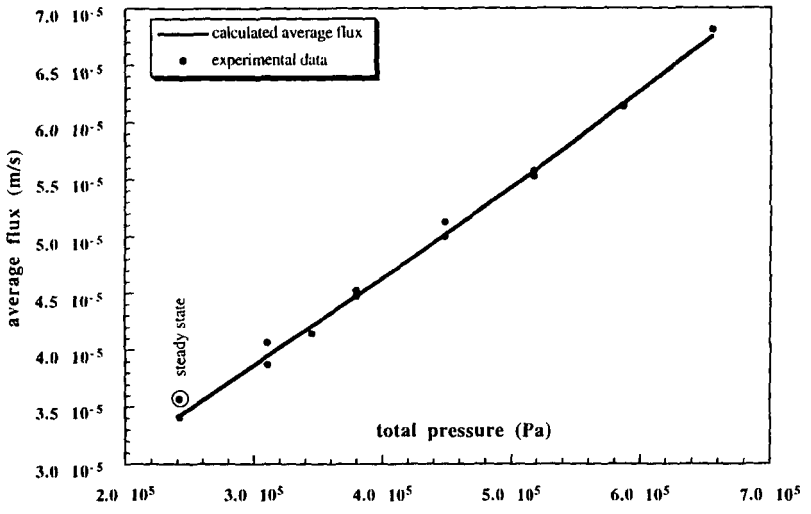

FIGURE 8. Average Flux Data for Steady-State and Pressure Excursion Points.

For the elevated pressure points of Figure 8 the flux will increase, but within a short duration there is minimal opportunity for accumulation or migration of the cake. As the load on the cake increases, so must the concentration; however, the amount of solute must remain fixed at each position. A new distribution of concentration will occur which maintains the amount of solute and balances the applied pressure against the hydraulic resistance.

The C(x,y) is sought in the implicit form $C(\sigma_{jj})$, where σ_{jj} is the local compressive stress from accumulated drag on the cake given by

$$\sigma_{jj} = -\int_{\infty}^{y} \frac{\partial P}{\partial y}\, dy \approx -\int_{\delta(x)}^{y} \frac{\partial P}{\partial y}\, dy. \tag{17}$$

The variation of $C(\sigma_{jj})$ should be subject to the observations from Porter's data, ($0.58 < C_c < 0.64$ at 0.138 MPa $\leq P \leq$ 0.641 MPa). Our transient analysis suggested 0.56 or 0.57 for the mean cake concentration at 0.241 MPa. Trial and

error methods were used to develop the $C(\sigma_{jj})$ shown in Figure 9. A sequence of approximations resulted in both the steady state and excursion fits indicated on Figure 8. Refinements less than 0.003 in concentration were not pursued.

Each symbol on Figure 9 represents conditions at intermediate locations along the membrane for the observed points shown on Figure 8. The point at concentration 0.54 and the group of points near the concentration 0.56 represent calculated concentrations at different locations on the membrane for the steady state condition. The average concentration for this operating point was 0.56 as earlier suggested from the transient calculations.

It is clear that the cake concentration is a function of the impressed pressure on the cake. The cake resistance begins at a concentration about 0.54 and the concentration increases to 0.65 asymptotically. At maximum pressure the concentration approaches the maximum random packing concentration of spherical particles (0.68).

The creeping velocity of the cake at the exit of the membrane can now be estimated from the cake thickness and concentration data. Figure 10 shows the creeping cake velocity as a function of the position in the cake. This velocity is only a few microns per second and the cake can be called a 'creeping' cake. The y-distance for the top of each curve yield the local cake thickness $\delta(x)$. The ratio of the length of the membrane to the creeping velocity yields a measure of the time required to purge cake assuming, perhaps counter the evidence (24), the fouling is reversible. With an average velocity of 3.5 μm per second at the exit plane of the membrane module, the cake will take about 18 hours to traverse the length of the membrane. The average creeping velocity increases with downstream distance and the mass flow rate of the cake is an increasing function with the downstream distance. It can be inferred that this creeping velocity will decrease with increasing transmembrane pressure as the cake gets compacted and its viscosity increases.

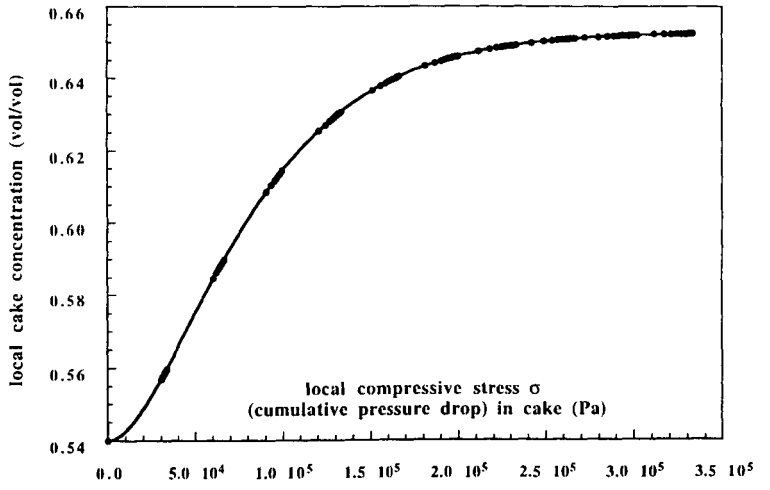

FIGURE 9. Dependence of Local Cake Concentration with Compressive Stress in Cake.

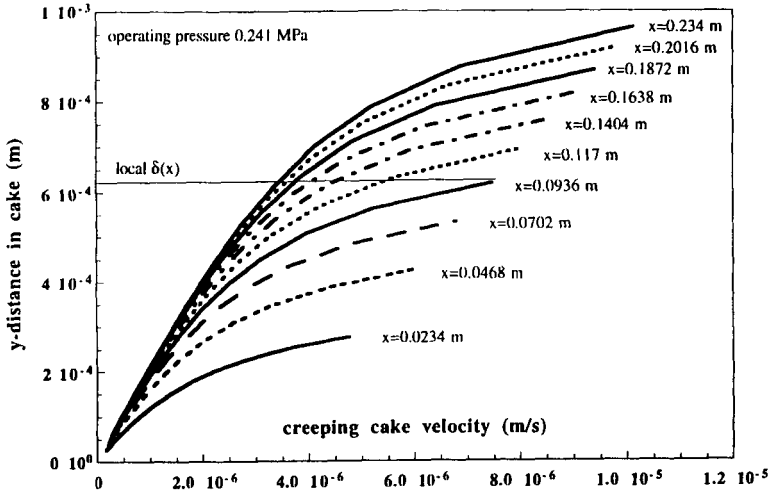

FIGURE 10. Velocity Profiles in Cake at Different Locations.

CONCLUDING REMARKS

It was shown that there are many models which estimate the lifting force (or suspension pressure) as function of the applied shear stress. It was seen that in most of the cases higher shear stress implied greater lifting force. From the magnitude analysis of these forces it was shown that for the operating parameters discussed herein, only the electrostatic force and the van der Waals attractive force are likely to be significant. These forces are in turn incorporated into a primary normal stress model derived from experimental reference. The fluid dynamic stresses are generally small compared to the transmembrane pressures, and so are significant only in the top few layers of the cake where the Kozeny-Carman drag pressure is in the same order of magnitude. For pressures beyond the level of dynamic stress, the cake becomes dense, supported by random contact (or near contact).

Experimental data by Porter (23) was found to indicate consistent behavior with the creeping cake hypothesis. The indicated average cake concentrations were shown to be affected by transmembrane pressures and shear stresses. This can be explained from a physical standpoint that higher pressure means higher cake compaction and vice versa. Increasing shear stresses generate increasing lift forces within the cake which suspend the particles in the cake, thus decreasing its concentration. However it was seen that the estimation of the actual viscosity is quite important and the solution is sensitive to its chosen value. The average cake concentration for Porter's data is in the range of random packing density of uniform spheres. Ultrafiltration experiments with a titania slurry also show that the cake concentrations are in the range of packing density of rigid, uniform non-interacting close packed spheres.

The mechanism of cake deposition was confirmed with experimental data under transient conditions. Continued experiments with a titania slurry under

steady-state conditions showed that the cake concentration is a function of the impressed pressure, as earlier suggested by Porter's data. After steady state was achieved, the flux was observed in a pressure excursion of short enough duration that the mass remained fixed. The entire set of steady state and fixed mass points were used to produce a concentration dependence on local compressive stress $C(\sigma_{jj})$. This $C(\sigma_{jj})$ together with the Kozeny-Carman model and measured viscosity in a force balance with mass conservation form a consistent model. The model allows the calculation of cake thickness distribution and the creeping velocity of the cake.

NOMENCLATURE

$A\beta$, $C\beta$	Constants (Table 3).
C, C(x,y),c	Cake concentration at any location (x,y) in cake.
C_0, $C_0(t)$	Bulk concentration of feed solution, initial bulk concentration.
C_c	Average volume concentration of cake.
c_{max}	Maximum possible concentration of the slurry at which its viscosity is infinite.
ΔP	Pressure drop (through a packed bed of spheres).
$\Delta P(x)_{total}$	Total transmembrane pressure drop.
$\Delta P(x,y)$	Pressure drop at any location of cake (x,y).
Δx	Incremental x.
h	Height of the control volume.
I(x,y)	See definition [Equation (9)].
J(x,t)	Transient flux at time t at any location x of the membrane.
J, J(x)	Permeate flux, steady state flux as a function of longitudinal distance of membrane.
$\bar{J}$	Length averaged mean flux value at steady state.

K	Kozeny-Carman constant (Equation 1).
K_A	Constant of AKHB Model (Equation 4),$\in$ (2,3).
L	Length of membrane.
m,n	Constants of shear-viscosity model for power law liquids (Equation 6).
N	Parameter of Wagner model (Equation 5).
P	Local Pressure.
R	Particle radius.
r	Cake resistivity (Equation 12).
R_m	Resistance of membrane ($\Delta P/J_0$).
t	Time.
u(x,y), U	Velocity of feed flow/creeping cake.
v_T	Velocity of flow at the top of the control volume.
x	Coordinate denoting longitudinal direction of feed flow.
y	Coordinate denoting perpendicular direction away from the membrane.

Greek Symbols

β, γ, γ_{ij}	Strain rate due to imposed shear stress, in direction i,j.
δ, $\delta(x,t)$	Thickness of fouling cake.
κ_D	Reciprocal of Debye length in solvent.
μ	General dynamic viscosity (slurry or solvent).
μ_0	Solvent dynamic viscosity.
μ_c	Cake viscosity at average cake concentration C_c.
μ_∞	Solvent dynamic viscosity at infinite strain rate.

σ	Surface charge density of solute particles.
σ_{jj}	Total compressive stress in cake in y direction.
τ, τ_{ij}	Shear stress, stress tensor in direction i,j.
Ψ_0	Surface charge potential.
Ψ_1	First normal stress coefficient (Equation 3a).
Ψ_2	Second normal stress coefficient (Equation 3b).

REFERENCES

1. A. L. Zydney, and C. K. Colton, "A Concentration Polarization Model for the Filtrate Flux in Cross-Flow Microfiltration of Particulate Suspensions.", Chem. Engr. Commun. 47, pp 1-21, (1987).

2. I. F. MacDonald, M. S. El-Sayed, K. Mow, and F. A. L. Dullien, "Flow Through Porous Media-the Ergun Equation Revisited.", Ind. Eng. Chem. Fundam., 87, No. 3, pp 199-208, (1979).

3. J. Happel, and H. Brenner, "Low Reynolds Number Hydrodynamics with a Special Application to Particulate Media.", Prentice-Hall, Inc., EngleWood Cliffs, N.J., (1965).

4. P. G. Saffman, "The Lift on a Small Sphere in a Slow Shear Flow.", J. Fluid Mech., 22, Part 2, pp 385-400, (1965).

5. G. Segré, and A. Silberberg, "Behavior of Macroscopic Rigid Spheres in Poiseuille Flow.", Part I and II, J. of Fluid Mech., 14, pp 115-157. (1962).

6. S. L. Soo, "Particles and Continuum, Multiphase Fluid Dynamics.", Hemisphere Publishing Corporation, New York, (1989).

7. S. I. Rubinow, and J. B. Keller, "The Transverse Force on a Spinning Sphere Moving in a Viscous Fluid.", J. Fluid Mech., 11, pp 447-459, (1961).

8. J. N. Israelachvili, "Intermolecular and Surface Forces.", Academic Press, (1992).

9. H. C. Hamaker, "The London-van der Waals Attraction Between Spherical Particles.", Physica IV, No. 10, pp 1058-1072, (1937).

10. R. Byron Bird, R. C. Armstrong and O. Hassager, "Dynamics of Polymeric Liquids." Vol 1, Fluid Mechanics, 2nd Edition, John Wiley & Sons. New York, (1987).

11. J. Statsna, D. De Kee, and M. B. Powley, "Modeling Complex Viscosity as a Response Function.", N. P. Cheremisinoff (Ed.), Encyclopedia of Fluid Mechanics, 7, Rheology and Non-Newtonian Flows, Gulf Publishing, (1986).

12. S. I. Abdel-Khalik, O. Hassager, and R. B. Bird, "Prediction of Melt Elasticity from Viscosity Data.", Polymer Eng. and Sci., 14, No. 12, pp 859-867, (1974).

13. M. H. Wagner, "Prediction of Primary Normal Stress Difference from Shear Viscosity Data Using a Single Integral Constitutive Equation.", Rheol. Acta., 16, pp 43-50, (1977).

14. H. L. Frisch, and R. Simka, "Viscosity of Colloidal Suspensions.", Rheology, Theory and Applications, 1, F. R. Eirick (Ed.), Academic Press Inc., New York, (1936).

15. H. N. Stein, "Rheological Behavior of Suspensions.", N. P. Cheremisinoff (Ed.), Encyclopedia of Fluid Mechanics, 5, Slurry Flow Technology, Gulf Publishing, (1986).

16. M. Mooney,"The Viscosity of a Concentrated Suspension of Spherical Particles.", J. of Coll. Sci., 6, pp 162-170, (1951).

17. J. M Krieger, "Rheology of Monodisperse Lattices.", Adv. Coll. Int. Sci., 3, pp 111-136, (1972).

18. D. Leighton, and A. Acrivos, "The Shear induced Migration of Particles in Concentrated Suspensions.", J. of Fluid Mech., 181, pp 415-439, (1987).

19. N. J. A. Sloane, "The Packing of Spheres.", Scientific American, January, pp 116-125, (1984).

20. W. M. Visscher, and M. Bolsterli, "Random packing of Equal and Unequal Spheres in Two and Three Dimensions.", Nature, 239, October 27, pp 504-507, (1972).

21. W. S. Jodrey, and E. M. Tory, "Computer Simulation of Isotropic, Homogeneous, Dense Random Packing of Equal Spheres.", Powder Tech., 30, pp 111-118, (1981).

22. K. Gotoh, W. S. Jodrey, and E. M. Tory, "A Random Packing Structure of Equal Spheres-Statistical Geometrical Analysis of Tetrahedral Configurations.", Powder Tech., 20, pp 233-242, (1978).

23. M. C. Porter, "Concentration Polarization with Membrane Ultrafiltration.", Ind. Eng. Chem. Prod. Res. Develop., 11, no 3, pp 234-248, (1972).

24. Y. K. Benkahla, A. Ould-Dris, M. Y. Jaffrin, and D. Si-Hassen, "Cake Growth Mechanism in Cross-Flow Microfiltration of Mineral Suspensions.", J. of Mem. Sci., 98, pp 107-117, (1995).